

Abnormal Bound Systems

Vladimir A. Karmanov 

Lebedev Physical Institute, Leninsky Prospect 53, 119991 Moscow, Russia; karmanovva@lebedev.ru

Abstract: It is taken for granted that bound systems are made of massive constituents that interact through particle exchanges (charged particles interacting via photon exchanges, quarks in elementary particles interacting via gluon exchanges, and nucleons in nuclei interacting via meson exchanges). However, as was recently theoretically found, there exist systems dominated by exchange particles (at least for the zero exchange masses). In these systems, the contribution of massive constituents is negligible. These systems have a relativistic nature (since they are mainly made of massless particles moving at the speed of light), and therefore, they cannot be described by the Schrödinger equation. Though these results were found so far in the simple Wick–Cutkosky model (spinless constituents interacting via the ladder of spinless massless exchanges), the physical ground for their existence seems to be rather general.

Keywords: Bethe–Salpeter equation; Wick–Cutkosky model; abnormal solutions; hybrid states

1. Introduction

Bound states have an essentially non-perturbative nature. They appear if the coupling constant exceeds some critical value (for an interaction of a finite radius). Their binding energies (and, therefore, the wave functions) cannot be calculated perturbatively. Let us consider, for example, a two-body system interacting with the Coulomb potential $V(r) = -\frac{\alpha}{r}$. Though, in this potential, the coupling constant α can take any small value (the bound states exist for any small α), the binding energy vs. α is quadratic: $E_n = -\frac{m\alpha^2}{4n^2}$, which already demonstrates its non-perturbative nature. If the perturbative correction to the free state in terms of the potential would be valid, in the first order, it should be linear vs. α . A non-perturbative solution implies that the scattering amplitude near the bound-state pole and binding energy are determined, in general, by the sum of infinite series in α , i.e., by an infinite number of exchanges. Then, a natural question arises: Why, in view of the infinite number of exchanges, are we dealing with a system containing massive constituents, not with a system containing, in addition to massive constituents, an indefinite (or even infinite) number of massless exchange particles?

We claim that the systems of both types are predicted by theory [1]. However, so far, we dealt mainly with non-relativistic systems, in which the effects of retardation in the interaction are not important. It is implied that the interaction is instantaneous. For this interaction, the lifetime of the virtual exchange particles in the system is zero (they are absorbed immediately after emission). Therefore, in its intermediate state, the system is dominated by slow (non-relativistic) particles. With the interaction approximated by a static potential, a few-body system is described by the Schrödinger equation. In this way, the intermediate states with many-body exchange particles are cut from the very beginning. This is a good non-relativistic approximation.

On the other hand, if systems of the second type (with many massless exchange particles in the intermediate states) exist, they should be described by a relativistic equation. Moreover, since a relativistic approach covers the full domain of momenta, both small and large, it can be applied to the systems of both types simultaneously: (i) the non-relativistic ones, also described



Citation: Karmanov, V.A. Abnormal Bound Systems. *Universe* **2022**, *8*, 95. <https://doi.org/10.3390/universe8020095>

Academic Editors: Chitta Ranjan Das, Alexander S. Barabash and Giuseppe Verde

Received: 6 December 2021

Accepted: 31 January 2022

Published: 3 February 2022

Publisher's Note: MDPI stays neutral with regard to jurisdictional claims in published maps and institutional affiliations.



Copyright: © 2022 by the author. Licensee MDPI, Basel, Switzerland. This article is an open access article distributed under the terms and conditions of the Creative Commons Attribution (CC BY) license (<https://creativecommons.org/licenses/by/4.0/>).

by the Schrödinger equation—the limiting case of the initial relativistic equation (the hydrogen atom in our case)—and (ii) purely relativistic systems, dominated by exchange particles, which cannot be discovered in the Schrödinger framework.

These qualitative considerations were recently confirmed by scrutinizing solutions of the relativistic Bethe–Salpeter (BS) equation. Though the story started almost 70 years ago with Wick and Cutkosky [2,3] solving the BS equation [4] for the spinless constituents interacting via the ladder of spinless massless exchanges, two types of solutions have been found.

One of them reproduced the normal Coulomb spectrum and wave function in the non-relativistic limit. The second one had no non-relativistic counterpart. It was absent in the Schrödinger equation, it was found in the BS equation, and it disappeared in the non-relativistic limit. Therefore, it was called “abnormal”. Its origin confused researchers and its nature was discussed in the literature over a couple of decades (see, e.g., §8 in [5] and references therein). In general, two irreconcilable hypotheses were put forward. (i) The abnormal solutions are a mathematical oddity of the BS equation. They have no physical sense. No physical system can be mapped to them. (ii) The abnormal solutions correspond to physical systems. They at least contribute to the S-matrix.

A breakthrough in understanding the abnormal solutions occurred after analyzing their content. It was found [1] that the valence contribution (of the massive constituents) is small and tends to zero when the binding energy decreases. Therefore, the abnormal states are dominated by the exchange particles. They can be called “hybrid systems”, as they contain a few constituents (two in the Wick–Cutkosky model considered below) and many exchange particles. This clarifies their nature.

The present paper is devoted to a review of these systems, which are dominated by massless exchange particles, as well as of their origins and properties. It is based on the results published in Ref. [1], as well as in our reports [6–8] at conferences. In Section 2, in the presentation of the field-theoretical background, we will not enter into the details of the formalized scheme. We will rely on a qualitative physical picture and designate only the outline. In the following sections, the presentation will be more precise. In Section 3, definition of the BS amplitude and its relation with the two-body wave function and the BS equation will be given. The method of solving the BS equation proposed by Wick and Cutkosky [2,3] is explained in Section 4. The origin of extra solutions of the BS equation found with this method (which are absent in the non-relativistic approach) is clearly demonstrated in Section 4. The two-body contributions to the full normalization of the state vector for the solutions of different natures are calculated in Section 5. The elastic and transition electromagnetic form factors for different solutions (both normal and abnormal) are presented in Section 6. The results are discussed in Section 7. Some technical details of calculating the full norm of the state vector are included in Appendix A.

2. The State Vector

It should be clarified that when we refer to the content of a physical system and its constituents, we imply that any system is described by the field-theoretical state vector $|p\rangle$. This state vector is an eigenstate of the Hamiltonian $H = H_0 + H_{int}$, where H_0 is the free Hamiltonian describing the free constituent and exchange fields, and H_{int} is the interaction between them. The four-momentum p is the momentum of the entire system. The eigenstates of the free Hamiltonian H_0 are the states $|n\rangle$ with a given number of the free constituent and exchange particles. The state vector $|p\rangle$ can be decomposed in terms of these free states $|n\rangle$ (as the bound-state wave function can be decomposed in the plane waves—the Fourier transform); each of them corresponds to a fixed (and different) number n . Schematically:

$$|p\rangle = \sum_n \psi_n |n\rangle. \quad (1)$$

A superposition of the states with different numbers of particles appears, since the interaction H_{int} does not conserve the number of particles. The state $|n\rangle$, which contains both “constituent” (valence) and “exchange” particles—a fixed number of them—is called the “Fock sector”, whereas the coefficients ψ_n of this decomposition, which correspond not only to a fixed number of particles, but also to their fixed momenta, are called the “Fock components”. According to the general rules of quantum mechanics, they determine the probabilities of finding n particles with momentum distributions of $|\psi_n|^2 \equiv |\psi_n(\vec{k}_1, \vec{k}_2, \dots, \vec{k}_n; \vec{p})|^2$ in the system described by the state vector $|p\rangle$. The integral over the momenta $\vec{k}_1, \vec{k}_2, \dots, \vec{k}_n$ determines the probability $N_n(\vec{p})$ of finding n particles in the system. The sum over n is normalized to 1:

$$\langle p|p\rangle = \sum_n N_n(\vec{p}) = 1. \quad (2)$$

In a non-relativistic two-body system, the probability N_2 of finding two constituent particles dominates (is practically equal to 1) and does not depend on p (it may differ from 1 due to relativistic corrections and the admixture of exchange particles). On the contrary, in this article, we will discuss the systems in which the sum that includes the exchange particles $\sum_{n>2} N_n$ dominates. Since $\sum_n N_n = 1$ and $N_n > 0$, this means that the probability N_2 of finding two constituents is small, whereas the average number of massless exchange particles can be large (maybe infinite). Referring to the content of the physical system, we just mean the probability of finding a given number of particles in this system.

Let us emphasize that after the integration of $|\psi_n(\vec{k}_1, \vec{k}_2, \dots, \vec{k}_n; \vec{p})|^2$ over momenta $\vec{k}_1, \vec{k}_2, \dots, \vec{k}_n$, the dependence on \vec{p} survives. That is, the probability $N_n(\vec{p})$ of finding n particles depends on the total momentum \vec{p} (it really depends on $|\vec{p}|$). It is different in different systems of reference. This is related to the fact that the dependence of the relativistic wave function $\psi_n(\vec{k}_1, \vec{k}_2, \dots, \vec{k}_n; \vec{p})$, where $\vec{k}_1 + \vec{k}_2 + \dots + \vec{k}_n = \vec{p}$, on the momenta is not reduced (in contrast to the non-relativistic one) to its dependence on the relative momenta. That is, the center-of-mass motion is not separated, which is in contrast to the non-relativistic wave function. From a physical point of view, the reason is the fact that in a relativistic system, the interaction is not instantaneous; aside from the constituents, there is an indefinite number of exchange quanta that are “in flight”. Therefore, the constituent coordinates do not determine the position of the center of mass in the momentum space, which implies the impossibility of introducing the relative momenta.

This can also be understood and confirmed from a more formal point of view. As with a non-relativistic wave function, the relativistic state vector $|p\rangle$ satisfies the eigenstate equation

$$H|p\rangle = M|p\rangle, \quad (3)$$

where M is the total mass of the system. This equation implies that the system is in the rest frame, that is, the four-vector p has the components $p = (M, \vec{0})$. Otherwise, the eigenvalue on the r.h.-side of this equation contains the total energy $E_p = \sqrt{M^2 + \vec{p}^2}$. The operator on the l.h.-side should be also determined; it is \hat{P}^0 , the zero-component of the four-momentum operator $\hat{P} = (\hat{P}^0, \hat{\vec{P}})$. That is, in an arbitrary reference frame, this equation should be written in the form of four equations, with a separate equation for each component of the four-momentum operator \hat{P} :

$$\hat{P}|p\rangle = p|p\rangle.$$

The interaction H_{int} enters into the operator \hat{P}^0 only; the operators $\hat{\vec{P}}$ are free.

As mentioned, in the decomposition (1), each term corresponds to a fixed number of particles, whereas the interaction does not conserve the number of particles—they can be virtually created and annihilated. In other words, the Hamiltonian H (and \hat{P}) does not commute

with the operator of the number of particles \hat{N} , which just results in the superposition (1) for its eigenvector $|p\rangle$.

Since the Fock components depend dynamically on \vec{p} , i.e., on the reference frame, one can try to find the most convenient reference frame. It turns out [9] that this reference frame is the infinite momentum frame $\vec{p} \rightarrow \infty$. Its convenience is determined by the following reason. In general, the virtual particles are created not only by their emission from constituents (as a process of their exchange), but as a result of vacuum fluctuations. A nucleon can virtually emit a meson: $nucleon \rightarrow nucleon + meson$. If so, the following virtual process is also possible: $vacuum \rightarrow nucleon + antinucleon + meson$ (or, e.g., $vacuum \rightarrow e^+e^-\gamma$). The advantage of the infinite momentum frame is in the fact that vacuum fluctuations do not exist in this frame. When $\vec{p} \rightarrow \infty$, their energy tends to infinity. Therefore, they are suppressed in the limit $\vec{p} \rightarrow \infty$ and do not contribute to the vacuum state vector. Hence, in the infinite momentum frame, the bare vacuum—an eigenstate of free Hamiltonian—is also an eigenstate of the Hamiltonian-containing interaction. This leads to very considerable simplifications, not only of the vacuum state, but of the whole theory.

The wave function in the infinite momentum frame is parametrized as follows. For brevity, we restrict ourselves to the two-body Fock component $\psi_2 = \psi_2(\vec{k}_1, \vec{k}_2; \vec{p})$. When we go to the reference frame with $\vec{p} \rightarrow \infty$, the transverse relative to the $\vec{p} \rightarrow \infty$ momenta $\vec{k}_{\perp 1,2}$ ($\vec{p} \cdot \vec{k}_{\perp 1,2} = 0$) does not vary with this transformation. We denote $\vec{k}_{\perp 1} \equiv \vec{k}_{\perp}$ ($\vec{k}_{\perp 2} = -\vec{k}_{\perp}$). Then, one introduces the ratios $x_{1,2} = \frac{k_{||1,2}}{p}$ (here, $\vec{k}_{||1,2} || \vec{p}$, $\vec{k}_{||1} + \vec{k}_{||2} = \vec{p}$) and denotes $x_1 \equiv x$, ($x_2 = 1 - x$), $0 \leq x \leq 1$. Therefore, in the limit $\vec{p} \rightarrow \infty$, the wave function in the infinite momentum frame is parametrized as $\psi_2 = \psi_2(\vec{k}_{\perp}, x)$. Its contribution to the normalization integral reads:

$$N_2 = \frac{1}{(2\pi)^3} \int |\psi_2(\vec{k}_{\perp}, x)|^2 \frac{d^2 k_{\perp} dx}{2x(1-x)}. \quad (4)$$

Here, N_2 is the limiting value of $N_2(\vec{p} \rightarrow \infty)$. The n -body Fock component is similarly parametrized (see, e.g., [10]).

These features can be described from a different, more formal and strict, but physically equivalent point of view. The Hamiltonian H mentioned above determines the evolution of the state vector from one moment of time to another. In the 4D Minkowski space, this is evolution from one plane $t = const_1$ to another $t = const_2$. So far, we discussed the state vector defined on the equal-time plane $t = const$. As is well known, two events that are simultaneous in one reference frame are not in equal time in other frame. Therefore, in addition to the plane $t = const$, one can introduce a space-like plane of general orientation, say, defined by the equation $\alpha t - \beta z = const$, and, instead of transformation from one plane $t = const_1$ to another plane $t = const_2$ (each in different moving reference frames), consider, now in the given reference frame, the state vector defined on the planes of different orientations (but still the space-like ones). One such plane differs from the other by the parameters α, β . The limiting case of the equal-time plane at $\vec{p} \rightarrow \infty$ for $\vec{p} || z$ corresponds to the light-front (LF) plane $t + z = const$ in this approach (it is enough to take $t + z = 0$). In this way, we come to the concept of LF dynamics in which the state vector is defined on the LF plane $t + z = 0$.

Another way to develop LF dynamics is to start with the LF Hamiltonian $\hat{P}^+ = \hat{P}^0 + \hat{P}^z$ instead of \hat{P}^0 and to consider the eigenstate equation in terms of this Hamiltonian. We obtain the same parametrization of the two-body Fock component $\psi_2 = \psi_2(\vec{k}_{\perp}, x)$ of the LF state vector.

If the state vector is defined on the equal-time plane $t = const$, we deal with the instant form of dynamics. The approach in which the state vector is defined on the plane $t + z = const$ is called the LF dynamics. Another form of dynamics in which the state vector is defined on the

hyperboloid $t^2 - \vec{x}^2 = \text{const}$ is called the “point form”. All three of these forms were introduced by Dirac [11]. The point form has also been successfully used in physical applications [12].

Note, however, that the formulation of LF dynamics on the plane $t + z = 0$ contains some inconvenience, since the 4D coordinates do not enter this formulation symmetrically. The coordinates t, z are distinguished compared to x, y . This violates the explicit relativistic covariance. The explicitly covariant form was developed in [13]. In this form, the LF hyperplane is determined by the equation $\omega \cdot x = 0$, where ω is a four-vector $\omega = (\omega_0, \vec{\omega})$ such that $\omega^2 = 0$; for a review, see [10]. In this version of LF dynamics, the explicit relativistic covariance is restored. The state vector still depends on the orientation of the LF plane, as it should. Now it is reduced to the dependence on the four-vector ω . The state vector should now be written as $|p, \omega\rangle$. This considerably simplifies the calculations, especially when incorporating spins of particles, such as when finding electromagnetic form factors. In the particular case $\omega = (1, 0, 0, -1)$, we come back to the ordinary version of LF dynamics.

Now, we can further define what we mean about the content of the system: We mean the Fock components integrated over momenta and squared $|\psi_n|^2$ for the state vector *defined on the LF plane*. For the two-body contribution, this integral is given by Equation (4).

3. Bethe–Salpeter Amplitude

Substituting the state vector $|p\rangle$ in the form of the decomposition (1) into the LF eigenstate equation $\hat{P}^+ |p\rangle = p^+ |p\rangle$, one obtains the system of the integral equations for the Fock components ψ_n . A convenient method of deriving this system is to use the LF graph technique presented in [10]. In many known cases, the convergence of the decomposition (1) for the LF state vector is rather fast, and it can be truncated with good accuracy [14,15]. After truncation, the system of equations for the Fock components becomes finite and can be solved numerically. One should properly carry out the renormalization. This approach has been developed in a series of articles; for a review, see [16].

However, if we expect that the system is dominated by a large number of exchange particles, this case is incompatible with fast convergence of the Fock decomposition. Another approach to the theory of relativistic bound systems [4] deals not with the state vector $|p\rangle$ itself and its Fock decomposition, but with the matrix element taken from the T-product of the Heisenberg operators between the vacuum state and the state $|p\rangle$, namely:

$$\Phi(x_1, x_2, p) = \langle 0 | T(\hat{\phi}(x_1) \hat{\phi}(x_2)) | p \rangle, \quad (5)$$

where $\hat{\phi}(x_{1,2})$ is the Heisenberg operator of the constituent field. The matrix element $\Phi(x_1, x_2, p)$ is the BS amplitude in the coordinate space. Sometimes, the amplitude defined by Equation (5) is called “the two-body BS amplitude”. To avoid misunderstandings, we would like to emphasize that this is, to some degree, slang reflecting the fact that this BS amplitude depends on two variables. The state vector $|p\rangle$ in the definition (5) contains all of the Fock components, including the many-body ones. Therefore, the BS amplitude (5) implicitly incorporates information not only about the two-body Fock sector, but also about the higher ones.

The transformation

$$\begin{aligned} \Phi(x_1, x_2, p) &= (2\pi)^{-3/2} \exp[-ip \cdot (x_1 + x_2)/2] \tilde{\Phi}(x, p), \quad x = x_1 - x_2, \\ \Phi(k, p) &= \int \tilde{\Phi}(x, p) \exp(ik \cdot x) d^4x, \end{aligned} \quad (6)$$

defines the BS amplitude $\Phi(k, p)$ in the momentum space. It satisfies the BS equation:

$$\Phi(k, p) = \frac{i^2}{[(\frac{p}{2} + k)^2 - m^2 + i\epsilon][(\frac{p}{2} - k)^2 - m^2 + i\epsilon]} \int \frac{d^4k'}{(2\pi)^4} iK(k, k', p) \Phi(k', p). \quad (7)$$

For one-boson exchange in the spinless case, the kernel reads:

$$iK(k, k', p) = \frac{i(-ig)^2}{(k - k')^2 - \mu^2 + i\epsilon}. \quad (8)$$

For massless exchange, one should put in (8) $\mu = 0$.

It turns out that by knowing the BS amplitude $\Phi(k, p)$, one can extract from it the two-body Fock component ψ_2 corresponding to two constituents. This possibility is provided by the fact that the Heisenberg operators turn, on the quantization plane, into the Schrödinger ones, which are free and constructed from usual creation and annihilation operators:

$$\hat{\phi}(x) = \frac{1}{(2\pi)^{3/2}} \int \left[a(\vec{k}) \exp(-ik \cdot x) + a^\dagger(\vec{k}) \exp(ik \cdot x) \right] \frac{d^3k}{\sqrt{2\epsilon_k}}. \quad (9)$$

This is true both for the equal-time case (when the Heisenberg operator $\hat{\phi}(x)$ on the plane $t = 0$ obtains the form (9)) and for the LF quantization (when the Heisenberg operator $\hat{\phi}(x)$ obtains the same form (9) on the LF plane $\omega \cdot x = 0$). However, of course, this is not simultaneous: If the Heisenberg operator obtains the form (9) on the LF plane, it has a very complicated form on the plane $t = 0$ that is not reduced to (9). Therefore, if both arguments of the BS amplitude $\Phi(x_1, x_2, p)$ are constrained by the LF plane $\omega \cdot x_1 = \omega \cdot x_2 = 0$, then for the operators $\hat{\phi}(x_{1,2})$, we can take Equation (9), and the product of the two annihilation operators $a(\vec{k}_1)a(\vec{k}_2)$ contained in $\hat{\phi}(x_1)\hat{\phi}(x_2)$ is contracted with the product of the two creation operators $a^\dagger(\vec{k}'_1)a^\dagger(\vec{k}'_2)$ contained in the two-body Fock sector of the state vector $|p\rangle$, and all of these operators disappear. The result is proportional to the two-body Fock component ψ_2 . The value of $\Phi(x_1, x_2, p)$ in the coordinate space with the arguments constrained to the LF plane $t_1 + z_1 = t_2 + z_2 = 0$ corresponds, in the momentum space, to the integral from $\Phi(k, p)$ over k_+ . In the explicitly covariant form, the relation between the BS amplitude $\Phi(k, p)$ and the two-body Fock component obtains the form:

$$\psi_2(\vec{k}_\perp, x) = \frac{x(1-x)}{\pi\sqrt{N_{tot}}} \int_{-\infty}^{\infty} dy \Phi\left(k + \frac{y\omega}{\omega \cdot p}, p\right), \quad (10)$$

where N_{tot} is the full normalization factor for a given state that provides the normalization condition $F(0) = 1$ of the elastic electromagnetic form factor for this state. The derivation of the relation (10) can be found in Ref. [10], Section 3.3. The values of N_{tot} in the limit of small binding energy for both normal and abnormal states are found analytically in Appendix A.

Solving the Equation (7) for the BS amplitude $\Phi(k, p)$, one can find, with Equation (10), the two-body Fock component ψ_2 , and then, with Equation (4), its contribution to the full norm of the state vector. Then, the contribution of the higher Fock sectors containing the exchange particles (in addition to the constituents) is $N_{n>2} = 1 - N_2$. Hence, in this way, we can calculate the full contribution of the exchange particles, but not the contributions of the particular Fock sectors containing them.

4. Solving the BS Equation in the Wick–Cutkosky Model

For the massless ladder exchange, i.e., for the kernel (8) with $\mu = 0$, Wick and Cutkosky [2, 3] reduced the BS Equation (7) to a one-dimensional equation that, in some limiting cases, can be solved analytically. The S-wave BS amplitude was represented in the form

$$\Phi_n(k, p) = \sum_{\nu=0}^{n-1} \int_{-1}^1 g_n^\nu(z) dz \frac{-im^{2(n-\nu)+1}}{\left[m^2 - \frac{1}{4}M^2 - k^2 - p \cdot k z - i\epsilon\right]^{2+n-\nu}}. \quad (11)$$

Here, n is an integer parameter, and the solutions exist for any $n = 1, 2, \dots$. Substituting (11) into the BS Equation (7) and following Ref. [3], one obtains the one-dimensional integral equation for $g_n^0(z)$:

$$g_n^0(z) = \frac{\alpha}{2\pi n} \int_{-1}^1 \frac{[R(z, z')]^n}{Q(z')} g_n^0(z'), \quad (12)$$

where α plays the role of the eigenvalue and is related to the coupling constant g in the kernel (8) as follows¹:

$$\alpha = \pi\lambda = \frac{g^2}{16\pi m^2}$$

and

$$R(z, z') = \begin{cases} \frac{1-z}{1-z'}, & \text{for } z' < z, \\ \frac{1+z}{1+z'}, & \text{for } z' > z, \end{cases} \quad (13)$$

$$Q(z) = 1 - \eta^2(1 - z^2), \quad \eta^2 = \frac{M^2}{4m^2}. \quad (14)$$

Namely, the single Equation (12) determines the mass spectrum. Other functions g_n^ν for the integer $0 < \nu \leq n - 1$ satisfy the system of inhomogeneous integral equations in which the inhomogeneous term is determined by $g_n^0(z)$. These equations, as well as Equation (12), can be transformed into the differential form. Together, along with Equation (11), they determine the BS amplitude $\Phi(k, p)$.

The key point revealing the mathematical origin of the abnormal solutions is the following. Just as the homogeneous Schrödinger equation can have a few (or even infinite) eigenvalues, the homogeneous Equation (12), for a given value of n and the coupling constant $\alpha > \frac{\pi}{4}$, also does not have a single solution, but an infinite set of eigenfunctions and corresponding binding energies [2,3]. To label them, an extra quantum number $\kappa = 0, 1, 2, \dots$ is introduced. The solution $g_{n\kappa}^0(z)$ with the mass $M_{n\kappa}^2$ vs. z has κ nodes within the interval $-1 < z < 1$ and a definite parity [3]:

$$g_{n\kappa}^0(-z) = (-1)^\kappa g_{n\kappa}^0(z).$$

Hence, the BS amplitude $\Phi(k, p)$ defined by Equation (11), which is taken in the rest frame as a function of the relative energy k_0 , is even or odd.

The odd solutions do not contribute to the S -matrix [17,18]. Therefore, we will mainly concentrate on the solutions with even κ , which may have a physical meaning.

A particular set of solutions with $\kappa = 0$ and arbitrary n , with a small binding energy $B_n \ll m$, reproduces the non-relativistic Coulomb spectrum [2,3] in the potential $V(r) = -\frac{\alpha}{r}$:

$$B_n = \frac{m\alpha^2}{4n^2}. \quad (15)$$

For the ground-state solution $n = 1$, for $B_1 \ll m$, Wick and Cutkosky [2,3] found $g_{10}^0(z) = 1 - |z|$. The corresponding two-body Fock component ψ_2 is expressed through the solution $g(z)$ below in Section 5. It is given by Equation (20). In the non-relativistic limit, it obtains the form (21) and coincides with the non-relativistic ground-state Coulomb wave function.

On the other hand, the solutions with non-zero $\kappa = 1, 2, \dots$ are completely decoupled from the non-relativistic solutions. They have a true relativistic nature and have no non-relativistic counterparts. These solutions are called “abnormal”.

In Figure 1, which was taken from Ref. [1], we show, in the Wick–Cutkosky model, the behavior of the coupling constant vs. the binding energy for a few of the lowest states with $n = 1$. The black solid line corresponds to $\kappa = 0$, whereas the black dashed line is the non-relativistic solution. With the increase in B , they deviate from each other due to the

relativistic correction, which is logarithmic. The colored solid lines correspond to $\kappa > 0$. The non-relativistic solutions that could be associated with them do not exist.

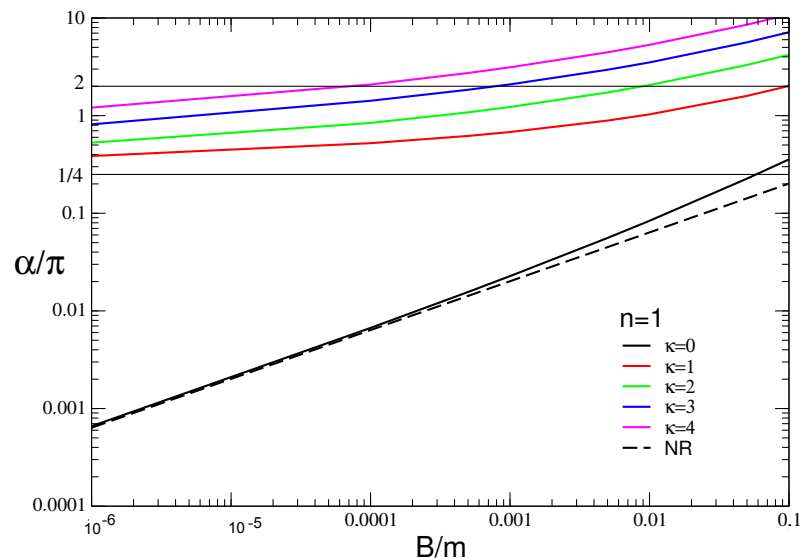


Figure 1. Spectrum in the Wick–Cutkosky model of the lowest coupling constants $\alpha(B)/\pi$ vs. κ for $n = 1$. The black solid line corresponds to $\kappa = 0$. The black dashed line is the non-relativistic solution. The colored solid lines correspond to $\kappa = 1 \div 4$. The horizontal line at $\alpha/\pi = 1/4$ corresponds to the minimal coupling constant for which the abnormal solutions exist. (Adapted from [1]).

For the small binding energy $B \rightarrow 0$, the following approximate formula for the spectrum of abnormal states with $\kappa = 2, 3, \dots$ was found [2,3]:

$$M_{n\kappa}^2 \simeq 4m^2 \left[1 - \exp \left(-\frac{(\kappa - 1)\pi}{\sqrt{\frac{\alpha}{\pi} - \frac{1}{4}}} \right) \right]. \quad (16)$$

It is evident that for real eigenvalues, the condition $\alpha > \pi/4$ must be satisfied. In this approximation ($B/m \ll 1$), the bound-state mass $M_{n\kappa}^2$ depends on κ only, but does not depend on n . If $\alpha \rightarrow \pi/4$, all of the abnormal excited energies tend to 0. In order for them to be distinguishable from the continuum, the coupling constant α should not be too close to $\pi/4$, but should be at least $\alpha \approx 4 \div 5$.

The binding energies for two normal ($n = 1, 2, \kappa = 0$) and four abnormal ($n = 1, 2, \kappa = 2, 4$) states found through the numerical solution of Equation (12) are shown in Table 1.

Table 1. Binding energy **B** (in units of m) for the quantum numbers $n = 1, 2$ and $\kappa = 0, 2, 4$. **N₂** is the contribution of these states to the full norm. The calculations were carried out for the coupling constant $\alpha = 5$. (Adapted from Tables 1 and 2 from [1]).

No.	n	κ	B	N ₂
1	1	0	0.999259	0.65
2	2	0	0.208410	0.61
3	1	2	3.51169×10^{-3}	0.094
4	2	2	1.12118×10^{-3}	0.077
5	1	4	1.54091×10^{-5}	6.19×10^{-3}
6	2	4	4.95065×10^{-6}	2.06×10^{-5}

One can see that even for $\alpha = 5$, the binding energies of abnormal states Nos. 3 ÷ 6 are rather small: $B \sim 10^{-3} \div 10^{-6}$ m relative to the normal ones. The normal states can have such small binding energies if they are extremely excited. Column N_2 , which shows the two-body contributions—the main subject of this review, together with the many-body one—will be discussed below.

The normal and abnormal solutions drastically differ in their behavior in the non-relativistic limit. The binding energy of normal solutions tends to a finite limit, whereas the abnormal solutions disappear—as mentioned, they have no non-relativistic counterparts. The latter means that in the non-relativistic limit, they are pushed out of the discrete spectrum. The non-relativistic limit means that all of the velocities are much smaller than the speed of light c , which, in the true non-relativistic realm, is considered as infinite. Therefore, it is convenient to find the non-relativistic limit by recovering the speed of light c (which was put to 1) in Equation (12) while considering c as a parameter and taking the limit $c \rightarrow \infty$. For this aim, we should introduce c in the input parameters, i.e., replace $m \rightarrow mc^2$, $\alpha = \frac{e^2}{\hbar c} \rightarrow \frac{\alpha}{c}$. We *should not* replace $M \rightarrow Mc^2$, since M is the output calculated with the c -dependent input parameters. The dependence of M (as well as the dependence of B) on c is determined by the equation. The dependence of the binding energy B on the speed of light c for the normal state $n = 1, \kappa = 0$ ($\alpha = 5$, No. 1 in Table 1 for $c = 1$) is given in Figure 2. It shows what happens with the binding energy in a smooth transition from the relativistic approach to the non-relativistic one.

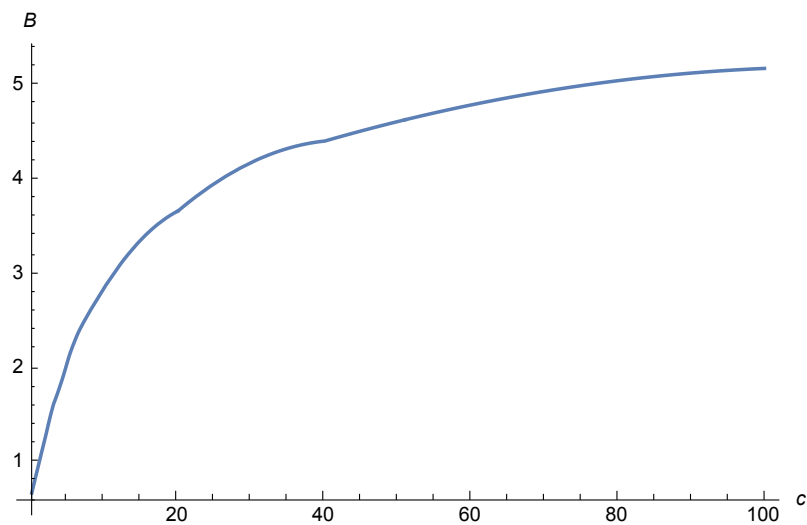


Figure 2. Dependence of the binding energy B of the state $n = 1, \kappa = 0$ (normal) for $\alpha = 5$ on the speed of light c .

This dependence is shown in Figure 3 for the case of the abnormal state $n = 1, \kappa = 2$ ($\alpha = 5$, No. 3 in Table 1 for $c = 1$).

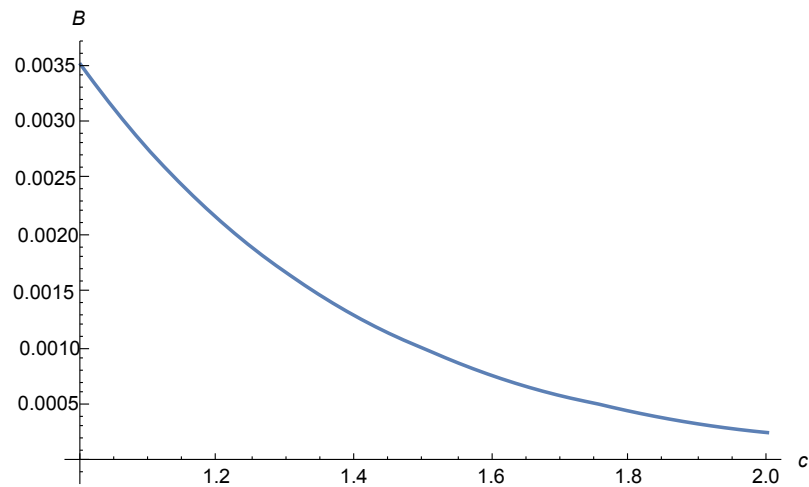


Figure 3. Dependence of the binding energy B of the abnormal state $n = 1, \kappa = 2$ for $\alpha = 5$ on the speed of light c .

At $c \rightarrow \infty$, in Figure 2, the binding energy of the normal state of the BS equation tends to be constant (which is given by the Schrödinger equation, i.e., by the Balmer series in Equation (15)). However, Figure 3 shows that the binding energy of the abnormal state has a quite different behavior: It decreases and tends to zero when c increases. That is, the abnormal state disappears in the non-relativistic limit.

The solutions for the $n = 1$ and $\kappa = 0, 2, 4$ states— g_{10}^0 , g_{12}^0 , and g_{14}^0 , arbitrarily normalized—are displayed in Figures 4–6.

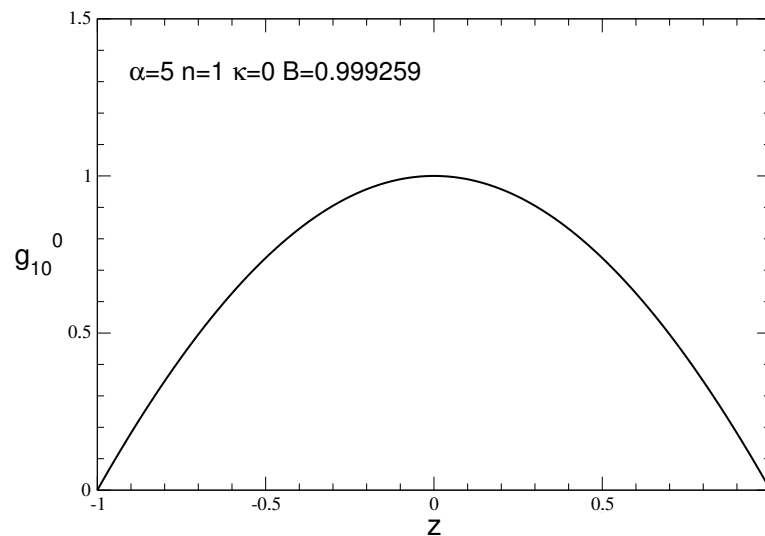


Figure 4. g_{10}^0 for state No. 1 ($\kappa = 0$, normal) from Table 1. (Adapted from [1]).

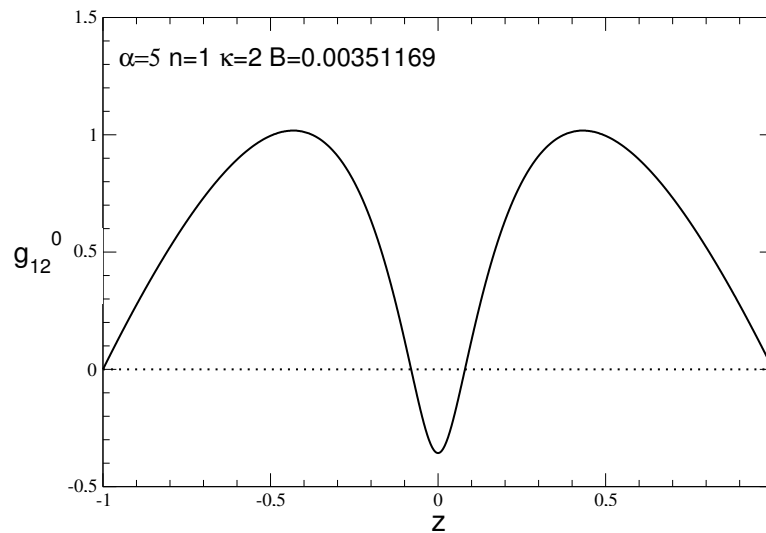


Figure 5. g_{12}^0 for state No. 3 ($\kappa = 2$, abnormal) from Table 1. (Adapted from [1]).

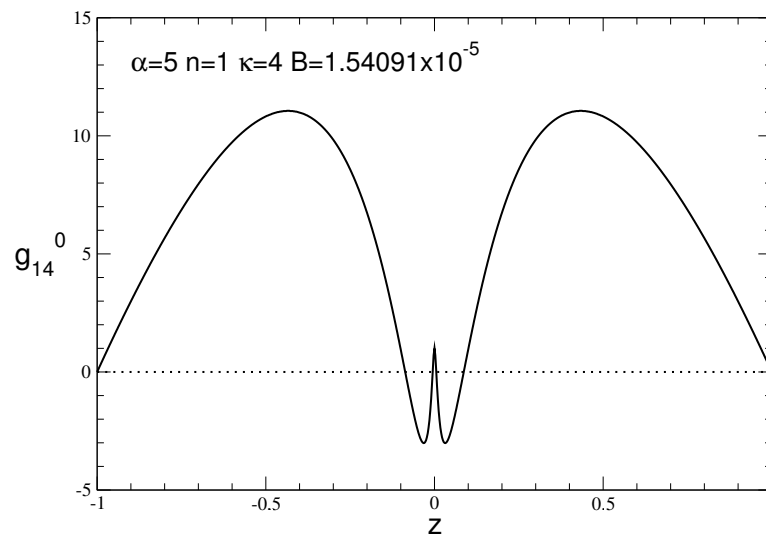


Figure 6. g_{14}^0 for state No. 5 ($\kappa = 4$, abnormal) from Table 1. (Adapted from [1]).

In Figures 4–6, we see that the number of nodes of each function $g(z)$ indeed coincides with the value of κ .

As mentioned, the functions $g_{n\kappa}^0(z)$ for $\nu = 0$ and for any n satisfy the Equation (12), which determines a series of eigenfunctions and binding energies labeled by the quantum number κ . For $n = 2$, the BS amplitude (11) contains another function $g_{2\kappa}^1$, corresponding to $\nu = 1$. The equation determining this function can be also found through the substitution of (11) into the BS equation (7). It has the form (see, e.g., [1]):

$$g_2^1(z) = \frac{\alpha}{6\pi} \int_{-1}^1 \frac{R(z, z')}{[Q(z')]^2} g_2^0(z') dz' + \frac{\alpha}{2\pi} \int_{-1}^1 \frac{R(z, z')}{Q(z')} g_2^1(z') dz'. \quad (17)$$

$R(z, z')$ and $Q(z')$ are defined in Equations (13) and (14). They are inhomogeneous relative to $g_2^1(z)$; the inhomogeneous term is determined by the function g_2^0 , which is known from Equation (12).

Then, the BS amplitudes for $n = 1, 2$ are expressed via these solutions, according to Equation (11), as:

$$\Phi_1(k, p) = \int_{-1}^1 \frac{-im^3 g_1^0(z) dz}{\left[m^2 - \frac{1}{4}M^2 - k^2 - p \cdot k z - i\epsilon\right]^3}, \quad (18)$$

$$\Phi_2(k, p) = \int_{-1}^1 \frac{-im^3 g_2^1(z) dz}{\left[m^2 - \frac{1}{4}M^2 - k^2 - p \cdot k z - i\epsilon\right]^3} + \int_{-1}^1 \frac{-im^5 g_2^0(z) dz}{\left[m^2 - \frac{1}{4}M^2 - k^2 - p \cdot k z - i\epsilon\right]^4}. \quad (19)$$

The system of equations for $g_{n\kappa}^\nu(z)$ with any n, ν is given in [1].

5. Two-Body Contributions

Knowing the BS amplitude $\Phi(k, p)$, we can find the two-body Fock component $\psi(\vec{k}_\perp, x)$ with Equation (10), and then, with Equation (4), we can find its contribution N_2 to the normalization of the full state vector. The difference $1 - N_2$ determines the contribution of the many-body Fock sectors with $n > 2$. With this method, the content of the normal states up to an extremely relativistic binding energy was analyzed in Ref. [19]. In [1], we applied this method to the abnormal states.

We substitute Equations (18) and (19) into Equation (10) and integrate over β . We omit the technical details of this integration, which can be found in Ref. [1], Appendix A. For $n = 1$ (ground state), the result reads:

$$\psi_{n=1}(\vec{k}_\perp, x) = \frac{m^3 x(1-x)g_1^0(1-2x)}{\sqrt{N_{tot}}[\vec{k}_\perp^2 + m^2 - x(1-x)M^2]^2} \quad (20)$$

We will show that in the non-relativistic limit, in appropriate variables, this wave function reproduces the ground-state hydrogen wave function. Instead of the pair of variables k_\perp, x , we introduce another pair q, θ with the formulas:

$$k_\perp = q \sin \theta, \quad x = \frac{1}{2} \left(1 - \frac{q \cos \theta}{\sqrt{m^2 + q^2}} \right).$$

Then, for $q \ll m$ and for the integration volume in (4), we obtain:

$$\frac{d^2 k_\perp dx}{2x(1-x)} = \frac{2\pi k_\perp dk_\perp dx}{2x(1-x)} = \frac{2\pi q^2 dq \sin \theta d\theta}{\sqrt{m^2 + q^2}} \approx \frac{2\pi q^2 dq \sin \theta d\theta}{m}.$$

We move the factor m from this denominator to the wave function, multiplying the latter by $1/\sqrt{m}$. Instead of M , we also introduce the binding energy B : $M = 2m - B$. As already indicated above, for $B \rightarrow 0$, $g(z) = 1 - |z|$, which gives $g_1^0(1-2x)|_{x \approx 1/2} \approx 1$. At last, for N_{tot} , we take expression (A2) from Appendix A. Then, the wave function (20) takes the form:

$$\psi_{n=1}(q) = \frac{8\sqrt{\pi}(Bm)^{5/4}}{(q^2 + Bm)^2}. \quad (21)$$

The wave function $\psi_{n=1}(q)$ (Equation (21)) is just the ground-state hydrogen wave function in the momentum space.

The normalization condition (4) turns into:

$$N_2 = \frac{1}{(2\pi)^3} \int \psi_{n=1}^2(q) 2\pi q^2 dq \sin \theta d\theta = 1. \quad (22)$$

Let us emphasize that the normalization condition (22) is not imposed, but derived. What is imposed (via condition $F(0) = 1$ applied to the electromagnetic form factor; see Section 6) is the normalization condition (2) for the full state vector. However, Equation (22) is a consequence of calculating the two-body wave function with Equations (10) and (20) and calculating N_{tot} with Equations (A1) and (A2). Its coincidence with 1 shows that, in the non-relativistic limit, the system consists of two constituents at 100%, as expected. As we will see below, it is not so for the relativistic states.

Similarly, for the first excited state $n = 2$,

$$\psi_{n=2}(\vec{k}_\perp, x) = \frac{m^3 x(1-x) g_2^1(1-2x)}{\sqrt{N_{tot}} [\vec{k}_\perp^2 + m^2 - x(1-x)M^2]^2} + \frac{2m^5 x(1-x) g_2^0(1-2x)}{3\sqrt{N_{tot}} [\vec{k}_\perp^2 + m^2 - x(1-x)M^2]^3}. \quad (23)$$

This wave function can be also transformed into the form of the solution of the Schrödinger equation with the Coulomb potential for the excited $n = 2$ state. Substituting the wave functions (20) and (23) into (4), we obtain the contributions of the two-body sectors for these states [1]:

$$N_2^{n=1} = \frac{1}{384\pi^2 N_{tot}} \int_{-1}^1 \frac{(1-z^2) [g_1^0(z)]^2 dz}{[Q(z)]^3}, \quad (24)$$

$$N_2^{n=2} = \frac{1}{3 \cdot 2^7 \pi^2 N_{tot}} \int_{-1}^1 dz (1-z^2) \left\{ \frac{[g_2^1(z)]^2}{[Q(z)]^3} + \frac{g_2^1(z) g_2^0(z)}{[Q(z)]^4} + \frac{4}{15} \frac{[g_2^0(z)]^2}{[Q(z)]^5} \right\} \quad (25)$$

with $Q(z)$ being defined in Equation (14).

The numerical results are given in the last column of Table 1. For the normal states, Nos. 1 and 2, the two-body contribution for $\alpha = 5$ is around 60%. This value, which considerably deviates from 100%, is related to the rather large binding energy ($B \sim 0.2 \div 1$ m) and, hence, to the considerable relativistic effects. The dependence of N_2 for the normal states $n = 1, 2, \kappa = 0$, on the binding energy B is presented in Figure 7.

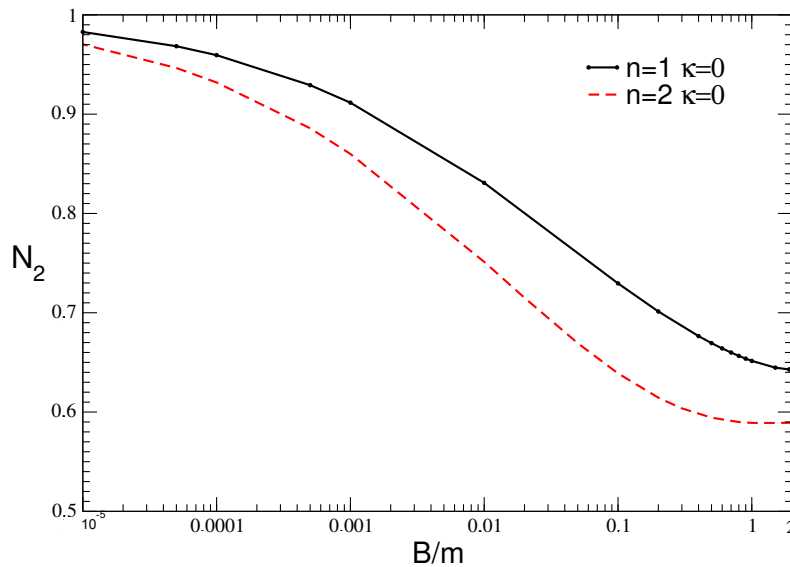


Figure 7. The two-body contribution N_2 vs. the binding energy B for the normal ($\kappa = 0$, $n = 1$, and $n = 2$) states. (Adapted from [1]).

For the abnormal state $n = 1, \kappa = 2$, as the calculations show, the value of N_2 increases with the increase in α . One can ask: Is it possible for some adequately large α to obtain an abnormal state that is not dominated by exchange particles, but with significant two-body content N_2 , say, 50%? It turns out that this is impossible: The abnormal states are always dominated by the exchange particles for any physically admissible values of the coupling constant α and the corresponding binding energies. With the increase in α , the squared ground-(normal-) state mass M^2 quickly decreases, and at $\alpha = 2\pi$, it reaches the value $M^2 = 0$. For larger α , M^2 becomes negative, and the system cannot be considered as the physical one. Though M^2 remains positive for the abnormal (excited) states, for such large values of α , these states (though with positive M^2) are the excited states of the physically senseless ground state with $M^2 < 0$, and therefore, in our opinion, they also have no physical meaning. For example, for the limiting value $\alpha = 2\pi$ ($M_{\text{ground}} = 0$), we find $B = 0.00903 m$ and $N_2 = 0.156$ for the first abnormal state. This is the maximal value of N_2 that can be achieved for the abnormal state. If we continue to increase α , then for $\alpha = 11$, we obtain $B = 0.059 m$ and $N_2 = 0.55 m^2$ for the abnormal state, i.e., an approximately 50–50% relation between the contributions of the constituent and exchange particles. However, the squared ground-state mass becomes $M^2 = -3.94 m^2$, so the system loses all physical meaning.

When $\alpha \rightarrow 0$, the constituent contribution for the ground state reads [19]:

$$N_2 = 1 - \frac{2\alpha}{\pi} \log \frac{1}{\alpha}.$$

When it is rewritten in terms of the binding energy, $B = \frac{1}{4}\alpha^2 m$, N_2 obtains the form:

$$N_2(B \rightarrow 0) = 1 + \frac{1}{\pi} \sqrt{\frac{4B}{m}} \log \frac{4B}{m} \quad (26)$$

On the contrary, as seen in Table 1, for the abnormal states, the two-body contribution is rather small: $N_2 \approx 10^{-1} \div 10^{-5}$ (for $n = 1, \kappa = 2$ and $n = 2, \kappa = 4$, respectively). The dependence of N_2 for the abnormal states $n = 1, 2, \kappa = 2$, on the binding energy B is shown in Figure 8.

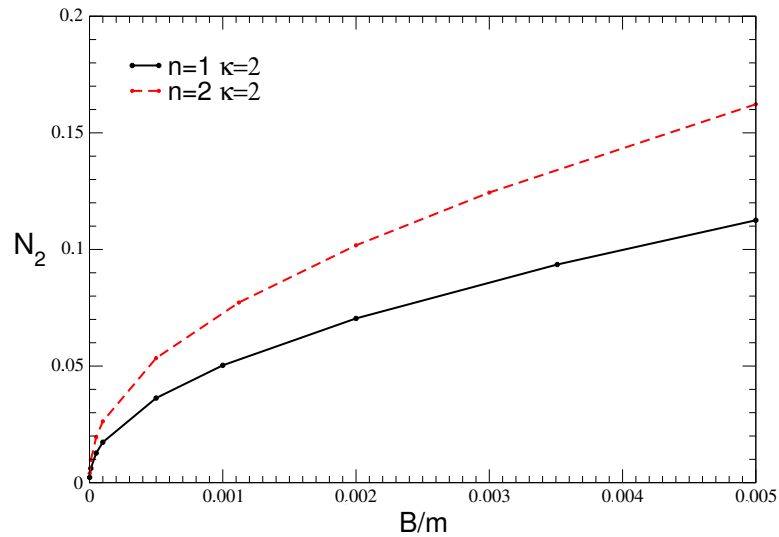


Figure 8. The two-body contribution N_2 vs. the binding energy B for the abnormal ($\kappa = 2$, $n = 1$, and $n = 2$) states. (Adapted from [1]).

For $B \rightarrow 0$, one can derive the analytical formula for N_2 for the abnormal states. For the particular case of $n = 1, \kappa = 2$, the derivation is given in Appendix A. The dominating term reads:

$$N_2(B \rightarrow 0) \propto \sqrt{\frac{B}{m}} \log^2 \frac{B}{m} \rightarrow 0. \quad (27)$$

This just reveals the nature of these states: The two-body valence contribution tends to zero, whereas the contributions containing the exchange particles dominate. Since the later many-body states, in addition to exchange particles, can contain valence ones, these states can be called hybrid states.

6. Elastic Electromagnetic and Transition Form Factors

The very different natures of the normal and abnormal states manifest themselves not only in their different contents (contributions of the valence and exchange particles), but also in the behaviors of their elastic electromagnetic form factors vs. the momentum transfer, as well as in the suppression of the transition form factors (transitions: the normal \rightarrow abnormal states) relative to the transitions between the states of the same nature. The asymptotic of the elastic form factors is determined by the nature of states: A fast decrease is a manifestation of a many-body structure [20–22].

We assume that one constituent particle is charged. Knowing the BS amplitude, one can calculate the electromagnetic form factor of the system. For generality, we will first consider the inelastic transitions from the factor between the different states $i \rightarrow f$. To find the elastic one, we put $f = i$.

First, we get the expression for the transition electromagnetic vertex J_μ . It is presented in the Feynman graph in Figure 9. The left and right vertex functions in this diagram are expressed through the BS amplitude. In this way, we obtain the following expression for J_μ in terms of the BS amplitude (compare with Equation (27) from [1] and with Equation (7.1) from [10]):

$$J_\mu = i \int (p + p' - 2k)_\mu \bar{\Phi}_f \left(\frac{1}{2} p' - k, p' \right) (k^2 - m^2) \Phi_i \left(\frac{1}{2} p - k, p \right) \frac{d^4 k}{(2\pi)^4}. \quad (28)$$

It can be decomposed in terms of two covariant structures:

$$J_\mu = \left[(p_\mu + p'_\mu) + (p'_\mu - p_\mu) \frac{Q_c^2}{Q^2} \right] F(Q^2) - (p'_\mu - p_\mu) \frac{Q_c^2}{Q^2} G(Q^2). \quad (29)$$

Here, $q = p' - p$, $Q^2 = -q^2 = -(p' - p)^2$, and $Q_c^2 = M_f^2 - M_i^2$, with M_i and M_f being the masses of the initial and final states, respectively. The scalar coefficients $F(Q^2)$ and $G(Q^2)$ in this decomposition are the form factors that we intend to calculate.

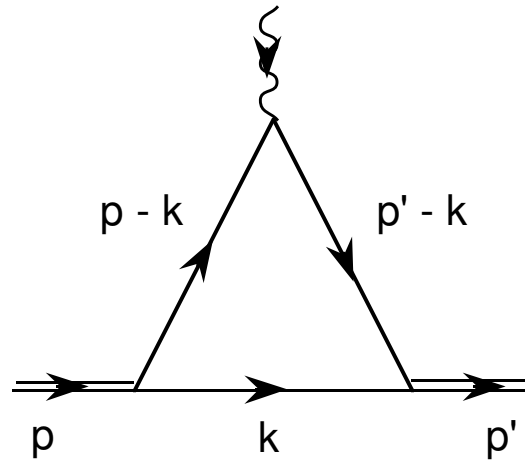


Figure 9. Feynman diagram for the electromagnetic form factor.

From Equation (29), one can find the expressions of the form factors:

$$F(Q^2) = \frac{(p + p') \cdot J Q^2 + q \cdot J Q_c^2}{[(M_f - M_i)^2 + Q^2][(M_f + M_i)^2 + Q^2]}, \quad G(Q^2) = \frac{q \cdot J}{Q_c^2}. \quad (30)$$

From the conservation of the electromagnetic current J_μ , which is expressed by the equality $q \cdot J = 0$, it follows that $G(Q^2) \equiv 0$ (for any Q^2). In Ref. [1], Appendix B, it is proven that this equality indeed follows from the BS equation. In other words, having found $\Phi(k, p)$ from the BS Equation (7), by substituting it into the current Equation (28) and extracting from it the form factor $G(Q^2)$ by means of Equation (30), we obtain zero. Below, we present the elastic form factors F for a few normal and abnormal states, as well as the inelastic ones for transitions between them.

We start with the form factors of the states corresponding to $n = 1$ and different κ s. The functions $g_{1\kappa}^0$ satisfy Equation (12), where one should put $n = 1$. The elastic form factor for the normal state with $n = 1, \kappa = 0$, $B = 0.999$ m—No. 1 of Table 1—is shown in Figure 10.

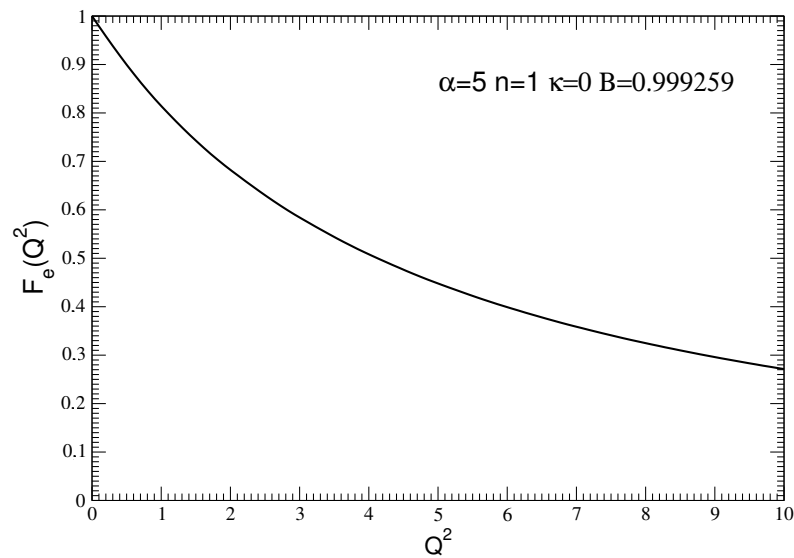


Figure 10. Elastic form factors for the normal state with $n = 1, \kappa = 0$ —No. 1 of Table 1. (Adapted from [1]).

The elastic form factors for the abnormal state with $n = 1, \kappa = 2, B = 0.00351$ m—No. 3 of Table 1—are shown in Figure 11 by the solid line. Comparing the solid curves in Figures 10 and 11, we see that the abnormal-state elastic form factor decreases, in the same interval of $0 \leq Q^2 \leq 1$, much faster (1000 times, approximately) than the normal one. There are a few reasons that are responsible for this faster decrease. Among them is the large size of the system due to the small binding energy, as well as its many-body content. In order to separate the many-body content, we adjust the value of α of state No. 1 so that it can have the same binding energy as that of state No. 3. The result is shown in Figure 11 by the dashed line. Though both curves have the same slope at the origin (that is, the systems have the same radii), the abnormal form factor still diminishes much faster than the normal one. At $Q^2 = 1$, the abnormal/normal ratio is approximately 1/10. This confirms the many-body content of the abnormal states.

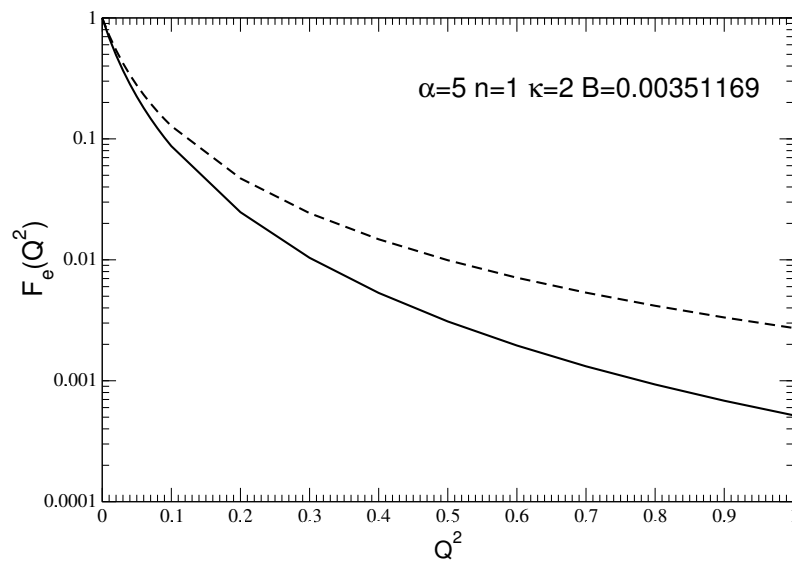


Figure 11. Solid line: abnormal elastic form factor of state No. 3 from Table 1 ($n = 1, \kappa = 2$). The dashed line is the normal elastic form factor of the state with $n = 1, \kappa = 0$ with the same binding energy (and, hence, rms radius) as for the solid line. (Adapted from [1]).

For the $n = 2$ states, the situation is analogous. The elastic form factor of the normal excited state in No. 2 with $n = 2, \kappa = 0$, and $B = 0.2084$ m is shown in Figure 12. Though it corresponds to a comparable binding energy, it decreases much faster (by one order of magnitude at $Q^2 = 1$) than the form factor for the state with $n = 1$ (No. 1), which is shown in Figure 10. It has two zeroes and becomes negative in the interval $Q^2 \in [1.5, 3.0]$. This reflects the complex structure of this system.

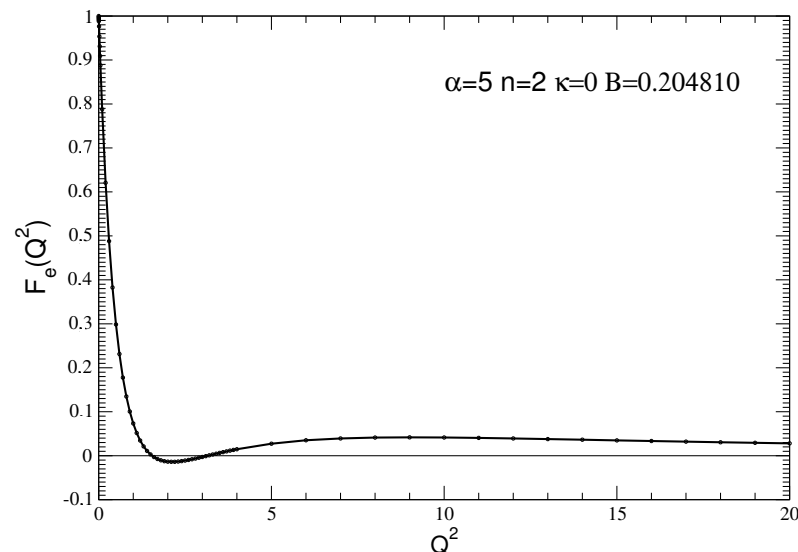


Figure 12. Elastic form factor of the normal excited state with $n = 2, \kappa = 0$ —No. 2 from Table 1. (Adapted from [1]).

Figure 13 represents the elastic form factor of the abnormal state ($n = 2, \kappa = 2, B = 0.00112$ m—No. 4 in the Table 1). It also decreases faster than the $n = 1, \kappa = 2$ state (No. 3) with a binding energy of the same order. Let us also emphasize the irregularity, which is

similar to that of a diffraction structure. Irregularities such as this one are normally absent in the ground-state form factors of two-body scalar systems. Their manifestation in the form factors of the excited state with $n > 1$ —both normal and abnormal—shows the complexity of these systems.

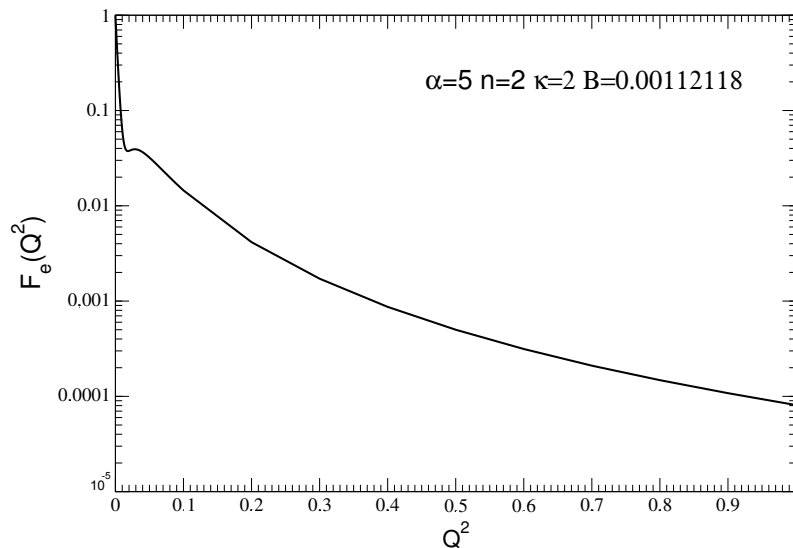


Figure 13. Elastic form factors of the abnormal state $n = 2, \kappa = 2$ —No. 4 of Table 1. (Adapted from [1]).

To reveal the influence of the quantum number n on the form factors and on their asymptotic, in Figure 14, we show the ratios of the form factors for the states with $n = 1$ and $n = 2$ and for the same fixed κ , either $\kappa = 0$ or 2. At large values of Q^2 , these ratios tend to the constant, which is the same (equal to ~ 7) for both ratios.

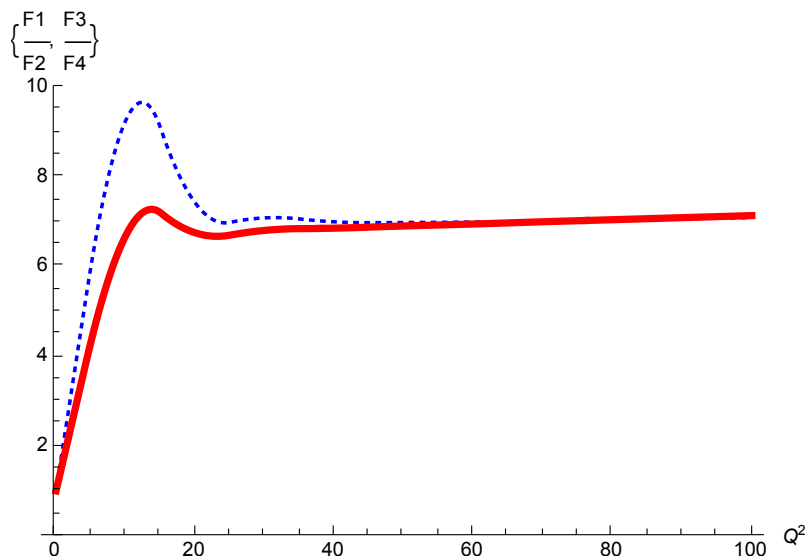


Figure 14. The ratios of the form factors for the states with $n = 1$ and $n = 2$. The dotted curve is the ratio for states Nos. 1 and 2 from Table 1, $\kappa = 0$. The solid curve corresponds to the ratio for states Nos. 3 and 4, $\kappa = 2$. (Adapted from [1]).

Note that the ratio of the abnormal/normal form factors also tends to be constant at large values of Q^2 ; however, this constant is much smaller than the normal/normal and

abnormal/abnormal ratios. This is seen in the comparison of Figure 14 with Figure 15. The latter figure shows the ratio of the abnormal/normal form factors (states Nos. 3 and 1). The value of the constant for the asymptotic of this ratio is $\sim 10^{-5}$.

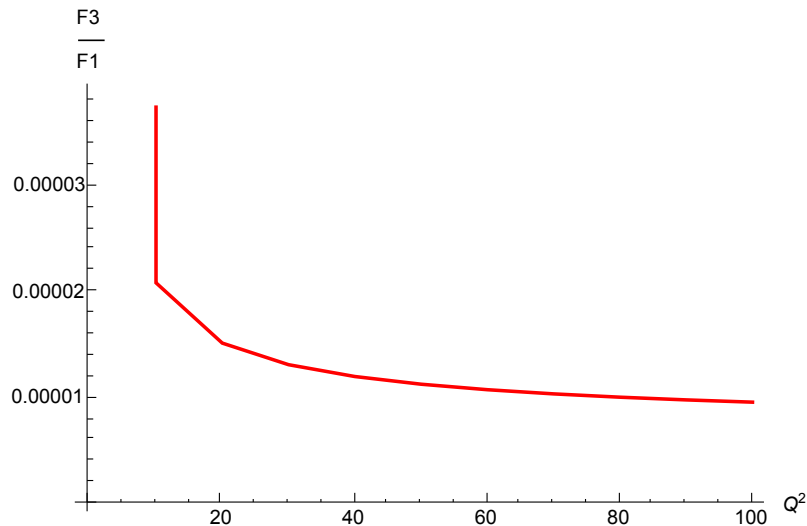


Figure 15. The form factor ratio: abnormal state No. 3/normal state No. 1 from Table 1. (Adapted from [1]).

Since the form factors decrease at different speeds for systems with different numbers of constituents, the fact that all of the form factor ratios shown in Figures 14 and 15 tend to be constants, though they are different for different states, supports the interpretation of the abnormal states as hybrid systems that contain both constituent (in small amounts) and exchange particles (dominant). Then, the asymptotic of the form factor is always determined by the two-body contributions, which are, however, very different for normal and abnormal states and are very small for the latter.

So far, we discussed the elastic form factors. The transition form factors are also very informative for understanding the structures of the abnormal states. We restrict ourselves to four states with $n = 1, 2; \kappa = 0, 2$ (Nos. 1 ÷ 4 in the Table 1). There are six transitions between four states. Figures 16 and 17 represent all six of these transition form factors.

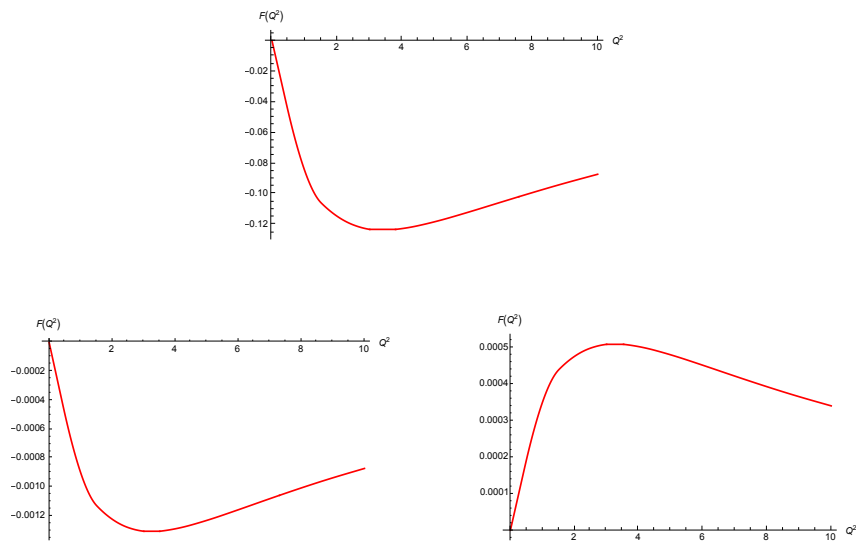


Figure 16. Form factors for the transitions from state No. 1 to the states with $\kappa = 0, 2$ listed in Table 1. (Adapted from [1]). Upper panel: normal (No. 1, $n = 1, \kappa = 0$) \rightarrow normal (No. 2, $n = 2, \kappa = 0$). Lower left panel: normal (No. 1, $n = 1, \kappa = 0$) \rightarrow abnormal (No. 3, $n = 1, \kappa = 2$). Lower right panel: normal (No. 1, $n = 1, \kappa = 0$) \rightarrow abnormal (No. 4, $n = 2, \kappa = 2$).

One can see that the transition form factors between the states of the same nature—normal–normal and abnormal–abnormal—are much larger than for the transitions between the states of different nature (normal–abnormal). Thus, the transition form factor between two normal states—No. 1 ($n = 1, \kappa = 0$) and No. 2 ($n = 2, \kappa = 0$), which are shown in the upper panel of Figure 16—is larger than the maximal values of the transition form factors from the normal to the abnormal states, which are shown in the lower panel, by a factor of ~ 100 .

The same property is confirmed by Figure 17. The maximal value of the transition form factor between two abnormal states—No. 3 ($n = 1, \kappa = 2$) and No. 4 ($n = 2, \kappa = 2$), which are shown in the upper panel of Figure 17—has the same order of magnitude as the normal–normal one shown in the upper panel of Figure 16. However, it decreases much faster with the increase in Q^2 . At the same time, this form factor is again larger than the maximal values of the transition form factors from the normal to the abnormal states, which are shown in the lower panels of Figures 16 and 17, by a factor of ~ 100 . These relations are apparently caused by the need to rebuild the structure of the system when the transition from a normal to an abnormal state takes place.

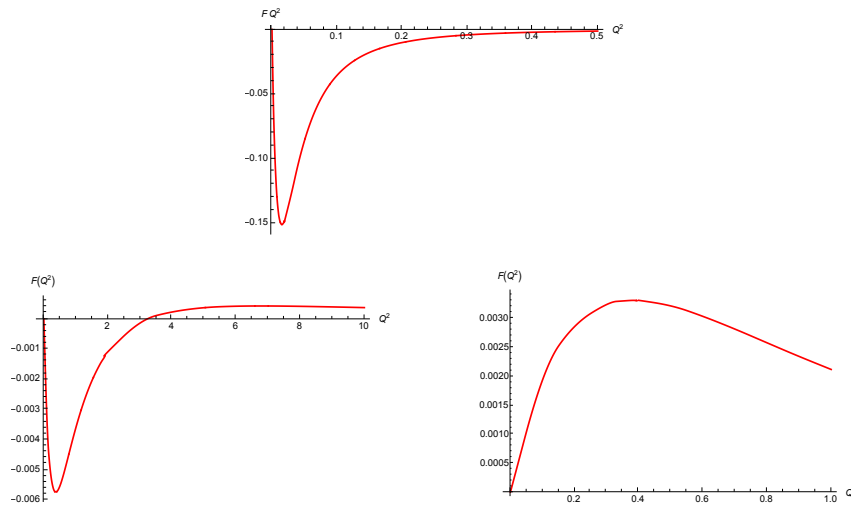


Figure 17. Transition form factors between the following states taken from Table 1. (Adapted from [1]). Upper panel: abnormal (No. 3, $n = 1, \kappa = 2$) \rightarrow abnormal (No. 4, $n = 2, \kappa = 2$). Lower left panel: normal (No. 2, $n = 2, \kappa = 0$) \rightarrow abnormal (No. 3, $n = 1, \kappa = 2$). Lower right panel: normal (No. 2, $n = 2, \kappa = 0$) \rightarrow abnormal (No. 4, $n = 2, \kappa = 2$).

Let us now come back to Equation (29) for the electromagnetic current. For the transitions, it contains an extra form factor $G(Q^2)$. This is determined by Equation (30). However, as mentioned, from the current conservation, it follows that $G(Q^2) \equiv 0$ for any Q^2 . A numerical check of this equality provides a strong test of the numerical calculations carried out in [1]. Therefore, together with the transition form factors presented above, the transition form factors $G(Q^2)$ were also calculated for all transitions.

The results are illustrated in Figure 18 with the example of the transition between state No. 2 ($n = 2, \kappa = 0$) and state No. 3 ($n = 1, \kappa = 2$). For the latter state, the BS amplitude is given by Equation (18), which contains one function, $g_1^0(z)$. For state No. 2, the BS amplitude is given by Equation (19), which contains a sum that includes two functions, $g_2^0(z)$ and $g_2^1(z)$. Therefore, the form factor $G(Q^2)$ is determined by the sum of two terms: $G^{00}(Q^2)$ (proportional to $g_2^0 g_1^0$) and $G^{10}(Q^2)$ (proportional to $g_2^1 g_1^0$). They are shown in Figure 18 by dotted ($G^{00}(Q^2)$) and dashed ($G^{10}(Q^2)$) lines, respectively. Their sum, that is, the full transition form factor $G(Q^2) \approx 10^{-6}$, is given by a thick solid line and is indistinguishable from zero on the scale of the figure. So, this test, which is extremely sensitive to any inaccuracy, is successfully satisfied. For example, a relative error in the calculation of the binding energy of the order of $\sim 10^{-4}$ destroys the cancellation seen in Figure 18. The value of $G(Q^2)$ takes on the order of the dashed and dotted curves.

The results of the calculations shown in Figures 10 and 12 for the normal states, as well as their comparisons with Figures 11 and 13 for the elastic abnormal form factors, clearly indicate that, with respect to Q^2 , the latter ones diminish considerably faster than the normal form factors. This affirms that abnormal bound systems are dominated by many-body Fock sectors [20–22].

The normal–abnormal transitions are considerably suppressed in comparison to the normal–normal and abnormal–abnormal ones. This is a manifestation of the fact that the normal and abnormal states have different levels of compositeness. Therefore, the normal–abnormal transitions entail the rebuilding of these states.

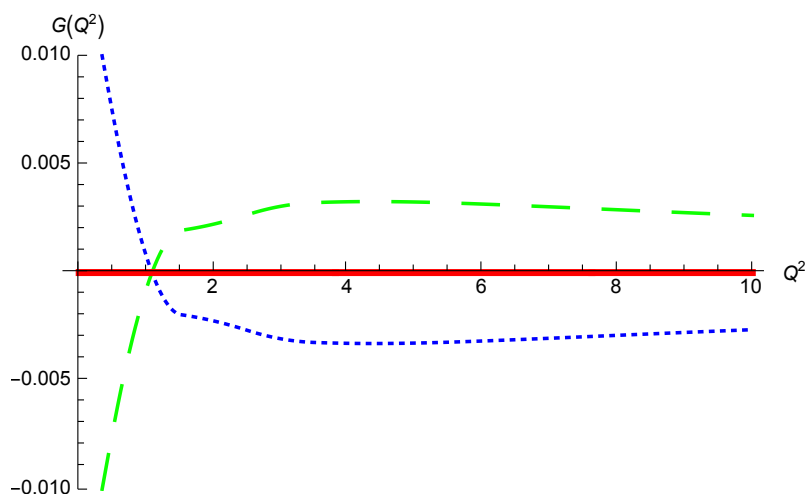


Figure 18. Contributions to the form factor $G(Q^2)$ of the transition between the states Nos. 2 and 3 from Table 1. The dotted line is $G^{00}(Q^2)$, and the dashed line is $G^{10}(Q^2)$ (for their definitions, see the text). The their sum (solid line) is the full form factor $G(Q^2)$. (Adapted from [1]).

7. Discussion

Our consideration is based on a conception that is widely used in nuclear and particle physics: Massive particles (constituents, valence particles) interact via exchanges with other light particles. We assume that the exchanges are massless. Traditionally, this model is applied to bound systems made of constituents. Indeed, in a static approximation, the interaction is reduced to the potential, and we deal with a non-relativistic system with a fixed number of constituents, as described by the Schrödinger equation.

We started this article with physical arguments supporting the existence of bound systems of quite different natures—relativistic systems dominated by exchange particles. There are two arguments (at least) in favor of this hypothesis: (i) the non-perturbative nature of bound states, which implies multiple exchanges; (ii) the manifestation of relativistic retardation effects in the propagation of exchange particles beyond the narrow domain of validity of the static approximation. These effects result in the filling of the intermediate states by the exchange particles, that is, in the appearance and domination in the state vector of the corresponding Fock sectors. Since two limiting cases (non-relativistic and ultra-relativistic) are associated with one and the same initial field-theoretical Hamiltonian, one can expect that they—if they exist—can be found from one and the same equation in its non-relativistic and fully relativistic domains.

This is exactly what was found by Wick and Cutkosky in their model [2,3]. For massless exchange, in the non-relativistic limit, they reproduced the ordinary Coulomb spectrum and the wave functions. In addition, they found new states that had no non-relativistic counterparts and that disappeared in the non-relativistic limit. The physical meaning of these new states remained unclear and controversial for a long time.

By analyzing the Fock sector content of both normal and abnormal states, we found [1,19] that the states of these two types drastically differ from each other. The normal states are dominated by constituent particles (as expected). On the contrary, the constituent contribution to the abnormal states is small. The latter have a different nature—they are dominated by exchange particles. The method that we use gives information about the probability of a two-body contribution, which is very small (see N_2 in Table 1, lines 3 ÷ 6), as well as information about the sum of the other ones (which dominate). This sum contains the contributions of “two constituents plus one exchange particle” + “two constituents plus two exchange particles”, etc.

However, we do not know the probability of each of these extra Fock sectors. However, the qualitative physical picture discussed in the introduction and the fast decrease in the elastic electromagnetic form factors (Section 6) speak in favor of the dominance of the Fock sectors of “two constituents plus many exchange particles”. This compositeness is also confirmed by a comparison of the values and behaviors of the form factors for the normal \rightarrow normal, abnormal \rightarrow abnormal, and normal \leftrightarrow abnormal transitions. The latter transitions require the rebuilding of the states, and therefore, they are especially suppressed.

For these reasons, we conclude that the abnormal states found in the BS framework correspond to bound systems of a relativistic origin that are dominated by massless exchange particles. They do not indicate a pathology in the BS equation (contrary to what is sometimes supposed in the literature).

The essentially non-perturbative origin of the abnormal states raises the question of the validity of the ladder approximation. The more important question is: Though a solvable model implies a simplified (ladder) kernel, are the abnormal states just a consequence of the ladder approximation? The multiparticle contributions to the BS kernel and their influence on the abnormal states have not been investigated. Since multiparticle Feynman graphs add extra particles in the intermediate states, one can expect that they increase the contributions of higher Fock sectors. It should at least be noted that the cross-ladder contribution to the ladder kernel increases the binding energy [23]. It increases the relativistic effects in the system and, therefore, should increase the many-body contributions. Therefore, it works in favor of, not against, the existence of the abnormal states.

In any case, although the Wick–Cutkosky model is oversimplified, it contains the phenomenon of intermediate particle creation, which is crucial for generating multiparticle Fock sectors. There are no indications that this generation is an artifact of ladder approximation. On the contrary, the generation of exchange particles in a bound system is a consequence of their creation in the intermediate kernel states and their manifestation in a relativistic system due to retardation. This phenomenon, even in the ladder kernel framework, provides an example of the natural formation of hybrid states. Therefore, one can expect that more complicated kernels and more sophisticated field theories also result in the formation of the states of this kind. However, since the binding energies of these systems are extremely small, the methods of their detection and the question of the “smoking gun” deserve special study.

The systems dominated by exchange particles can have an electromagnetic nature. However, in view of the results discussed above, we also mention glueballs and hybrid states predicted in QCD (for a review, see [24–26] and the references therein). In principle, glueballs originate for different reasons, such as self-interactions of gluons. They do not contain constituent quarks. However, the states considered in the present article have a hybrid nature—they appear due to exchanges between constituents. However, as we saw, the contribution of the Fock component containing the constituents only tends to zero for small binding energies. In addition, we considered scalar massless colorless exchanges, where the problem of the color compositeness of hybrid states does not appear. However, glueballs made of colored gluons must be colorless. This imposes restrictions on their compositeness. In our opinion, these differences, however, can be considered as secondary. Generally, the main reason for the origination of systems dominated by massless particles is the possibility of easy virtual creation of the latter in the intermediate states, independently of the particular mechanisms of their creation: self-interaction or exchanges between constituents in the ladder approximation or beyond it. From this general point of view, the states discussed in the present article and glueballs can be considered as being akin to each other.

So far, we discussed the results found in the case of massless exchange particles. Research on the case of massive exchange particles is in progress.

Funding: This research received no external funding.

Conflicts of Interest: The author declares no conflict of interest.

Abbreviations

The following abbreviations are used in this manuscript:

BS Bethe–Salpeter
LF Light front

Appendix A. Calculating N_{tot} in the Limit $B \rightarrow 0$

For any given state, the expression for N_{tot} at $B \rightarrow 0$ in terms of the solution $g(z)$ corresponding to this state is found from the condition $F_{el}(0) = 1$, where $F_{el}(Q)$ is the elastic form factor of this state. It is determined by Equation (A.11) from [1]:

$$N_{tot}(B \rightarrow 0) = \frac{3m^{5/2}}{2^6 \pi B^{5/2}} \int_0^1 dz' \int_0^1 dz \frac{z^2 z'^2 g(z) g(z')}{(z + z')^5}. \quad (\text{A1})$$

For the normal $n = 1$ state, one has $g(z) = 1 - |z|$ [2,3,5]. Substituting this into (A1) and integrating over z, z' , we find:

$$N_{tot}(B \rightarrow 0) = \frac{m^{5/2}}{2^{10} \pi B^{5/2}}. \quad (\text{A2})$$

The substitution of this expression into (24) results in $N_2(B \rightarrow 0) = 1$ with the correction determined by Equation (26).

For abnormal states with $\kappa \geq 1$ —still in the limit $B \rightarrow 0$ —the solution reads [2,3,5]:

$$g_{\kappa n}(z) = (1 - z^2)^n |z|^{\frac{1}{2} + \rho} F\left(\frac{1}{2}\left(\frac{3}{2} + \rho + n\right), \frac{1}{2}\left(\frac{1}{2} + \rho + n\right), n + 1; 1 - z^2\right), \quad (\text{A3})$$

where F is the hypergeometric function, $\lambda = \frac{\alpha}{\pi}$,

$$\rho = \sqrt{\frac{1}{4} - \lambda}, \quad \lambda = \frac{1}{4} + \frac{\pi^2(\kappa - 1)^2}{\left[\log\left(1 - \frac{1}{4}M^2\right)\right]^2}.$$

The two-body contribution is given by Equation (24). It contains $Q^3 \approx \left(z^2 + \frac{B}{m}\right)^3$ in the denominator. Therefore, the integral (24) for N_2 is determined by the domain $z \rightarrow 0$. In this domain and for $\rho \rightarrow 0$, the solution (A3) for $n = 1, \kappa = 2$ takes the form:

$$g_{21}(z) \approx -\frac{4\sqrt{2z}}{\pi} \left(2 + \log \frac{z}{8}\right).$$

Then, by calculating N_2 , we find for the leading term:

$$N_2(B \rightarrow 0) \approx \frac{\log^2 \frac{B}{m}}{96 B^2 N_{tot}} \quad (\text{A4})$$

N_{tot} is given by Equation (A1), where $g(z)$ is determined by Equation (A3) with $n = 1, \kappa = 2, \rho \rightarrow 0$. The dependence on B is determined by the factor $1/B^{5/2}$, whereas, in this case, the double integral cannot be calculated analytically, but is calculated numerically: $N_{tot}(B \rightarrow 0) \approx 8 \times 10^{-4} (m/B)^{5/2}$. By substituting this expression into Equation (A4), we obtain Equation (27) for the abnormal $N_2(B \rightarrow 0)$.

Note

- ¹ Do not confuse the coupling constant g with the function $g_n^{\nu}(z)$ in the decomposition (11) and with the solution $g_n^0(z) \equiv g_n^{\nu=0}(z)$ of Equation (12).

References

- Carbonell, J.; Karmanov, V.A.; Sazdjian, H. Hybrid nature of the abnormal solutions of the Bethe–Salpeter equation in the Wick–Cutkosky model. *Eur. Phys. J. C* **2021**, *81*, 50.
- Wick, G.C. Properties of Bethe–Salpeter wave functions. *Phys. Rev.* **1954**, *96*, 1124–1134.
- Cutkosky, R.E. Solutions of a Bethe–Salpeter equation. *Phys. Rev.* **1954**, *96*, 1135–1141.
- Salpeter, E.E.; Bethe, H. A Relativistic equation for bound-state problems. *Phys. Rev.* **1951**, *84*, 1232–1242.
- Nakanishi, N. A General survey of the Bethe–Salpeter equation. *Prog. Theor. Phys. Suppl.* **1969**, *43*, 1–81.
- Karmanov, V.A.; Carbonell, J.; Sazdjian, H. Bound states of relativistic nature. In Proceedings of the International Conference: Nuclear Theory in the Supercomputing Era-2018 (NTSE-2018), Daejeon, Korea, 29 October–2 November 2018; Shirokov, A.M., Mazur, A.I., Eds.; Pacific National University: Khabarovsk, Russia, 2019; p. 212. Available online: <http://ntse.khb.ru/files/uploads/2018/proceedings/Karmanov.pdf> (accessed on 24 January 2022).
- Karmanov, V.A.; Carbonell, J.; Sazdjian, H. Bound states of purely relativistic nature. *EPJ Web Conf.* **2019**, *204*, 01014. <https://doi.org/10.1051/epjconf/201920401014>.
- Karmanov, V.A.; Carbonell, J.; Sazdjian, H. Structure and EM form factors of purely relativistic systems. In Proceedings of the Light Cone 2019—QCD on the Light Cone: From Hadrons to Heavy Ions, Ecole Polytechnique, Palaiseau, France, 16–20 September 2019; Volume 374, p. 50.
- Weinberg, S. Dynamics at Infinite Momentum. *Phys. Rev.* **1966**, *150*, 1313–1318.
- Carbonell, J.; Desplanques, B.; Karmanov, V.A.; Mathiot, J.-F. Explicitly Covariant Light-Front Dynamics and Relativistic Few-Body Systems. *Phys. Rep.* **1998**, *300*, 215–347.
- Dirac, P.A.M. Forms of Relativistic Dynamics. *Rev. Mod. Phys.* **1949**, *21*, 392–399.
- Klink, W.H.; Schweiger, W. Point form relativistic quantum mechanics. In *Relativity, Symmetry, and the Structure of Quantum Theory*; Morgan & Claypool Publishers: San Rafael, CA, USA, 2018; Volume 2.
- Karmanov, V.A. The wave functions of relativistic bound systems. *Sov. Phys. JETP* **1976**, *44*, 210–219.
- Li, Y.; Karmanov, V.A.; Maris, P.; Vary, J.P. Ab Initio Approach to the Non-Perturbative Scalar Yukawa Model. *Phys. Lett. B* **2015**, *748*, 278–283.
- Karmanov, V.A.; Li, Y.; Smirnov, A.V.; Vary, J.P. Nonperturbative solution of scalar Yukawa model in two- and three-body Fock space truncations. *Phys. Rev. D* **2016**, *94*, 096008.
- Mathiot, J.-F.; Smirnov, A.V.; Tsirova, N.A.; Karmanov, V.A. Nonperturbative renormalization in light-front dynamics and applications. *Few-Body Syst.* **2011**, *49*, 183–203.
- Ciafaloni, M.; Menotti, P. Operator analysis of the Bethe–Salpeter equation. *Phys. Rev.* **1965**, *140*, B929–B946.
- Naito, S. S-matrix and abnormal solutions of the Bethe–Salpeter equation. *Prog. Theor. Phys.* **1968**, *40*, 628–639.
- Hwang, D.S.; Karmanov, V.A. Many-body Fock sectors in Wick–Cutkosky model. *Nucl. Phys. B* **2004**, *696*, 413–444.
- Matveev, V.A.; Muradyan, R.M.; Tavkhelidze, A.N. Automodellism in the large-angle elastic scattering and the structure of hadrons. *Lett. Nuovo Cim.* **1973**, *7*, 719–723.
- Brodsky, S.J.; Farrar, G.R. Scaling laws at large transverse momentum. *Phys. Rev. Lett.* **1973**, *31*, 1153–1156.
- Radyushkin, A. Quark counting rules: Old and new approaches. *Int. J. Mod. Phys. A* **2010**, *25*, 502–512.
- Carbonell, J.; Karmanov, V.A. Cross-ladder effects in Bethe–Salpeter and Light-Front equations. *Eur. Phys. J. A* **2006**, *27*, 11–21.
- Klempt, E.; Zaitsev, A. Glueballs, hybrids, multiquarks: Experimental facts versus QCD inspired concepts. *Phys. Rep.* **2007**, *454*, 1–202.
- Mathieu, V.; Kochelev, N.; Vento, V. The Physics of Glueballs. *Int. J. Mod. Phys. E* **2009**, *18*, 1–49.
- Ochs, W. The status of glueballs. *J. Phys. G* **2013**, *40*, 043001.